AUT Journal of Electrical Engineering

AUT J. Elec. Eng., 50(1)(2018)101-106
DOI: 10.22060/eej.2017.11922.5016

Distorted Reflector Antennas: Radiation Pattern Sensitivity to the Surface Distortions

A. Haddadi*, A. Ghorbani

Department of Electrical Engineering, Amirkabir University of Technology, Tehran, Iran

ABSTRACT: The high-frequency performance of the reflector antennas is mainly limited by the surface. It has been shown that distortions on different regions of the reflector surface can have different effects on the radiation performance. In other words, degradation of the radiation pattern due to the presence of surface distortions is sensitive to the location and behavior of the surface distortion profile. In this paper, the concept of "sensitivity of the radiation pattern to the surface distortion" has been introduced and quantified. It can be used in the design of different reflector antennas to prevent radiation degradations due to surface distortion. Based on the Physical Optics and variational analysis, the first-order variational of the far-fields with respect to the surface profile is formulated to present the concept of sensitivity. The variational amplitude can be modified to show the concept of sensitivity of the radiation pattern to the distortions on the surface. Reflector antennas with different geometries and feeding methods have different sensitivity plots. Both co- and cross-polarization fields for feed antenna are considered ti be used in the symmetric and offset reflectors, and sensitivity plots are extracted. Sensitivity plots show areas on the surface that have stronger effects on the radiation pattern variations in the region of the main-lobe and the first few side-lobes.

Review History:
Received: 27 August 2016
Revised: 29 April 2017
Accepted: 21 June 2017
Available Online: 15 August 2017

Keywords:
Reflector antenna
surface distortion
offset reflector antenna

1- Introduction

High-gain, wide-band, and low-cost characteristics of a reflector antenna makes it the best candidates for satellite, radar and imaging applications [1]. In the region of the main beam and the first few side-lobes, which is the region of interest in high-gain applications, Physical Optics (PO) method is accurate [2].

There are two types of inaccuracies on reflector surface: random surface errors (or simply, surface errors) and systematic distortions (or surface distortions) [3]. Surface distortions result from thermal, gravitational, dynamical, and other effects, while surface errors are made by inaccuracies in the manufacturing process. However, these inaccuracies can degrade the reflector antennas' radiation performance [4]. Ruze presented a useful statistical model to determine the average pattern and gain loss due to surface errors [5]. Also, there are some works that analyze the effects of surface errors on the cross-polarization level, side-lobe level, and pattern shape [6-8].

In the presence of systematic surface distortions, distortion profile plays a key role in deviation of the far-field pattern. In many works, some known deterministic surface distortion functions are considered and their effects on the radiation characteristics of the antenna has been studied. Radiation characteristics can be on-axis gain, side-lobe level, cross-polarization level, or radiation pattern [4, 9-11]. However, results are limited to a specific type of distortion or radiation characteristic.

The corresponding author; Email: abolfazl.haddadi@gmail.com

Smith presents a relationship between radiation pattern and surface distortion by expanding an exponential phase error function for the first and second order approximation. Also, the reflector surface can be discretized into different triangular areas and the contribution of each area to the radiation field can be linearized as in [9] and [12].

Authors have developed a new formulation based on the variational techniques to relate the surface distortions and radiation pattern variations [14-15]. Based on PO approximation, the first variational of the radiation field is extracted in a general form. Consideration of the normal vector deviation contributions in the final results makes the formulation capable to be applied for both slow-varying and fast-varying distortions. The formulation is applicable to each polarization component (co- or cross-polarized) of radiated field. The sensitivity of the radiation field variations with respect to distortions on different regions of the reflector surface can be quantified and displayed to show regions with stronger effects on radiation pattern. Different feed polarizations (linear or circular) are considered to study the effects of feed polarization on the radiation pattern for distorted reflectors. Here, the variational amplitude plots are interpreted as "sensitivity of the radiation pattern to the surface distortions". To the best knowledge of the authors, the concept of the radiation sensitivity to surface distortion has not been studied in other works.

In Section II, the first variational for radiation field is extracted. Variational amplitudes, which can determine the regions with the strongest effect on the radiation fields, are plotted for different case studies, and discussions are provided in section III. Finally, Section IV gives some concluding remarks.

2- Formulation

Fig. 1 shows the description of the reflector surface and the feed antenna in the global coordinate system $\{\hat{x},\hat{y},\hat{z}\}$. The feed radiation pattern can be defined in its own local coordinate system $\{\hat{x}_f,\hat{y}_f,\hat{z}_f\}$. To relate these coordinate systems, Eulerian angles and translation vectors can be used. The position vectors of the reflector surface points are in primed vectors.

2- 1- PO approximation and radiation integral

Based on PO approximation for surface current and using a surface integral to double integral conversion, the complex far-field function for the reflector antenna is [16]

$$\bar{G}(\theta,\phi)=\frac{\eta}{j2\lambda}\int_{\psi=0}^{2\pi}\int_{t=0}^{1}\bar{N}\times\bar{H}^{\text{inc}}\ e^{jk\bar{r}'\cdot\hat{r}}\,\mathrm{d}t\,\mathrm{d}\psi \tag{1}$$

with λ the wavelength, η the free space impedance, $\bar{r}'$ the position vector for points on the reflector surface, and $\hat{r}$ the observation unit vector along (θ,ϕ) direction are defined as

$$\bar{r}'(\theta,\phi)=\sin\theta\cos\phi\hat{x}+\sin\theta\cos\phi\hat{y}+\cos\theta\hat{z}. \tag{2}$$

Moreover, $\bar{H}^{\text{inc}}$ is the incident magnetic field radiated by feed antenna. Vector $\bar{N}$ is along the surface normal vector and is calculated by [10]

$$\bar{N}=\left(\frac{\partial x'}{\partial t}\hat{x}+\frac{\partial y'}{\partial t}\hat{y}+\frac{\partial z'}{\partial t}\hat{z}\right)\times\left(\frac{\partial x'}{\partial\psi}\hat{x}+\frac{\partial y'}{\partial\psi}\hat{y}+\frac{\partial z'}{\partial\psi}\hat{z}\right) \tag{3}$$

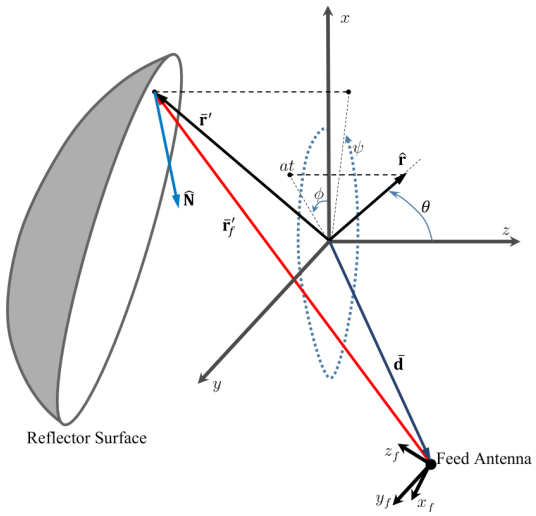

Fig. 1 Antenna geometry and the coordinate systems for the feed and the reflector.

where $x'=x'(t,\psi)$, $y'=y'(t,\psi)$, $z'=z'(t,\psi)$ are functions to describe surface points' coordinates in aperture plane parameters t and ψ. More details on the formulations are provided in [15].

2- 2- Functional interpretation of radiation integral

A functional $F[f]$ is the mapping of function $f(x)$ defined over some interval $x\in[a,b]$ and a number F that generally depends on the values of the function over all points of the interval [17]. The vector $\bar{G}$ in (1) can be interpreted as a functional of function $z(t,\psi)$ with two variables (t,ψ)

$$\bar{G}=\bar{G}[z(t,\psi)]=\frac{\eta}{j2\lambda}\int_{\psi=0}^{2\pi}\int_{t=0}^{1}\bar{g}(t,\psi;z,z_t,z_\psi)\,\mathrm{d}t\,\mathrm{d}\psi \tag{4}$$

where $z(t,\psi)$ with respect to t and ψ, respectively, and vector $\bar{g}$ is defined as

$$\bar{g}=\bar{N}\times\bar{H}^{\text{inc}}\ e^{jk\bar{r}'\cdot\hat{r}} \tag{5}$$

Taylor expansion for functional $\bar{G}[z]$ in (4) can be extracted,

$$\bar{G}[z+\Delta z]=\bar{G}[z]+\frac{\eta}{j2\lambda}\int_{\psi}\int_{t}\frac{\delta\bar{G}[z]}{\delta z(t,\psi)}\Delta z(t,\psi)\mathrm{d}t\,\mathrm{d}\psi \tag{6}$$

where $\frac{\delta\bar{G}[z]}{\delta z(t,\psi)}$ is the first variational of functional $\bar{G}[z]$ with respect to function $z(t,\psi)$.

In [17], it is shown that the first variational can be calculated as [17]

$$\frac{\delta\bar{G}[z]}{\delta z(t,\psi)}=\frac{\partial\bar{g}}{\partial z}-\frac{\mathrm{d}}{\mathrm{d}t}\frac{\partial\bar{g}}{\partial z_t}-\frac{\mathrm{d}}{\mathrm{d}\psi}\frac{\partial\bar{g}}{\partial z_\psi} \tag{7}$$

where operators ∂ and d denote partial and total derivation, respectively. With some mathematical manipulations on (4) and (5), it can be shown that first variational equation in (7) can be rewritten as [15]

$$\frac{\delta\bar{G}[z]}{\delta z(t,\psi)}=jk\left[a^2t\left(\hat{r}-\hat{r}_f'\right)+\left(\bar{N}-a^2t\hat{z}\right)\left(\hat{z}\cdot\hat{r}_f'\right)\right]\times\bar{H}^{\text{inc}}\ e^{jk\bar{r}'\cdot\hat{r}} \tag{8}$$

where a is the radius of the aperture and $\hat{r}_f'$ is the position unit vector with respect to feed coordinate system origin and is obtained by

$$\hat{r}_f'=\frac{\bar{r}'-\bar{d}}{\left|\bar{r}'-\bar{d}\right|}. \tag{9}$$

$\bar{d}$ is the position vector for the phase center of the feed antenna. It should be noted that since in the calculation of variational we need to consider first derivations, the effects of deviations in the normal vector of the reflector surface are included.

2- 3- Variational Amplitude

The variational equation in (8) can show each surface point's contribution to the distortion of the radiation fields. It means that one can specify regions on the surface that have stronger effects on the radiation field when the distortion exists in those regions. This can be valuable during the design or the manufacturing of the reflector surfaces. In the next section, some plots are presented to display the amplitude of the vector $\frac{\delta\bar{G}[z]}{\delta z(t,\psi)}$ for each polarization component.

The variational formula in (8) is independent of the distortion profile. It is only dependent on the parameters from the undistorted surface and the observation vector $\hat{r}$, i.e. (θ,ϕ). For a point on the surface with coordinates of (t,ψ), a function can be defined as

$$\gamma_p(t,\psi;\theta,\phi)\equiv\eta\hat{p}^*\cdot\frac{\delta\bar{G}[z]}{\delta z} \tag{10}$$

where $\hat{p}$ is the unit polarization vector. In the Ludwig's third definition, this vector is given by [16]

$$\hat{p}_{\mathrm{H}} = \cos\phi\hat{\theta} - \sin\phi\hat{\phi} \tag{11a}$$

$$\hat{p}_{\mathrm{V}} = \sin\phi\hat{\theta} + \cos\phi\hat{\phi} \tag{11b}$$

$$\hat{p}_{\mathrm{R}} = e^{-j\phi}\left(\hat{\theta} - j\hat{\phi}\right)/\sqrt{2} \tag{11c}$$

$$\hat{p}_{\mathrm{L}} = e^{+j\phi}\left(\hat{\theta} + j\hat{\phi}\right)/\sqrt{2} \tag{11d}$$

for vertical, horizontal, right-handed, and left-handed circular polarization, respectively.

he definition in (10) is such that the variation of the far-field function, say $\Delta G_p(\theta,\phi)$, due to surface distortion function $\Delta z(t,\psi)$ would be

$$\Delta G_p(\theta,\phi) = \int_{\psi=0}^{2\pi}\int_{t=0}^{1} \gamma_p(t,\psi;\theta,\phi)\frac{\Delta z(t,\psi)}{\lambda}\,\mathrm{d}t\,\mathrm{d}\psi \tag{12}$$

The function $\gamma_p(t,\psi;\theta,\phi)$ can be interpreted as the radiation field variation due to surface deviation $\Delta z(t,\psi)$ (with respect to wavelength) at point (t,ψ) on the surface. However, as this function varies with θ and ϕ, it is of value to define a parameter as

$$\Gamma_p^{\theta_m} \equiv \max\left\{\left|\gamma_p(t,\psi;\theta,\phi)\right|; \forall\,\theta<\theta_m, 0\le\phi\le 2\pi\right\} \tag{13}$$

de contribution of the surface point (t,ψ) to the radiation fields inside the region $\theta<\theta_m$. More side-lobes can be considered by increasing θ_m. Here, $\theta_m = 6\lambda/2\pi \approx 6\,HPBW\,rad$ is selected to consider main-beam and the first two side-lobes

3- Results

As for case studies, different offset reflector antennas with circular aperture are considered with diameter $2a$, focal length F, and offset length H, and a feed antenna with $\cos^q\theta$ radiation pattern in different polarization states and the edge taper is located at the focal point. Considering Fig. 1, we have $\bar{d} = -H\hat{x}$.

Design parameters for four case studies are listed in Table 1. First three cases are offset, and the last case is symmetrically-fed (zero offset). Also, the first and second cases have the same parameters, but with different feed polarization. Both circular and linear polarization are used.

The normalized values of $\Gamma_{\mathrm{co}}^{3\lambda/4}(t,\psi)$ and $\Gamma_{\mathrm{cr}}^{3\lambda/4}(t,\psi)$ for the undistorted antenna are calculated in each case. Each plot is normalized to its maximum value. The contours could show the regions that have more effect on the radiation fields when a distortion is applied in those regions.

A. Case study 1

We consider the offset reflector antenna as case study 1, that is adapted from [10]. The feed antenna has -12dB edge-taper (q =14.28), and it radiates a x–polarized (Horizontal) field.

The normalized $\Gamma_{\mathrm{H}}^{2.83^\circ}(t,\psi)$ and $\Gamma_{\mathrm{V}}^{2.83^\circ}(t,\psi)$ are plotted in Fig. 2, and contours show that the left half of the reflector (the lower half in the Fig 1) has more effect on the radiation in the presence of distortions. The maximum position(s) for the co-polar and cross-polar component is located at $(x=-0.636a, y=0)$, and $(x=-0.264a, y=\pm 0.763a)$, respectively.

Table 1. Reflector antenna parameters for Different Case studies

Parameter	Case Study 1	Case Study 2	Case Study 3	Case Study 4
Diameter $2a$	$60.7060\lambda_0$	$60.7060\lambda_0$	$40\lambda_0$	$25\lambda_0$
Focal Length F	$59.989\lambda_0$	$59.989\lambda_0$	$32\lambda_0$	$10\lambda_0$
Offset Height H	$49.5925\lambda_0$	$49.5925\lambda_0$	$30\lambda_0$	0
Feed Edge Taper ET	−12dB	−12dB	−15dB	−20dB
Co-polar component	Horizontal	Vertical	RHCP	LHCP

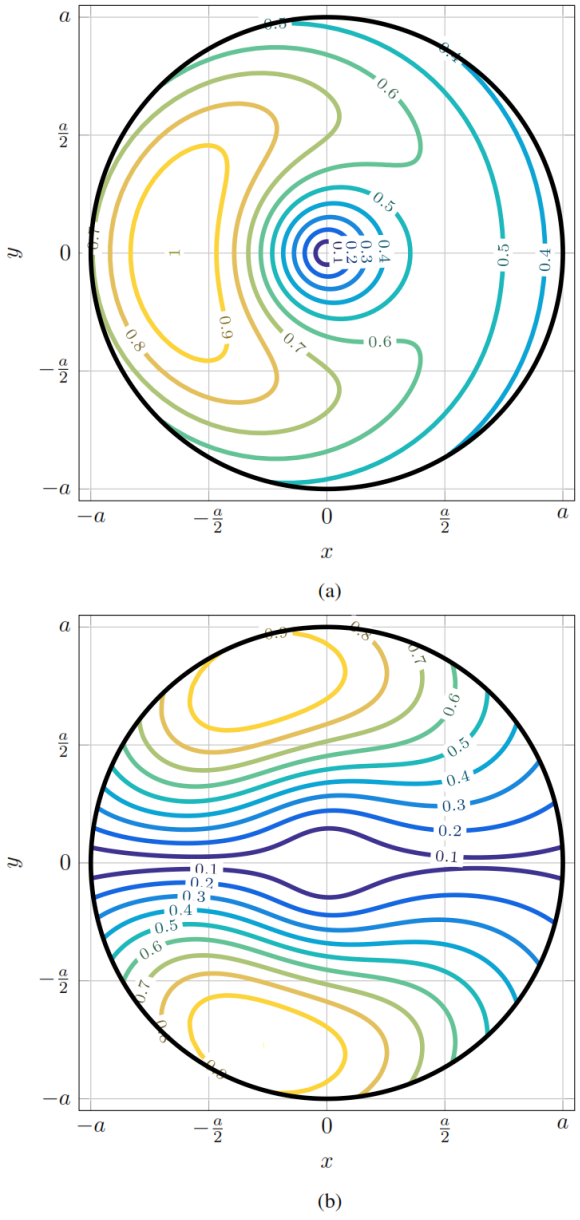

Fig. 2 Normalized variational amplitudes, (a) $\Gamma_{\mathrm{H}}^{2.83^\circ}(t,\psi)$, (b) $\Gamma_{\mathrm{V}}^{2.83^\circ}(t,\psi)$, for case 1.

B. Case study 2

The same offset reflector antenna as the latter case is considered as case study 2, with a different feed with a *y*- polarized (Vertical) radiation field. Thus, the co-polar component is vertical here.

The normalized $\Gamma_{\mathrm{V}}^{2.83^\circ}(t,\psi)$ and $\Gamma_{\mathrm{H}}^{2.83^\circ}(t,\psi)$ are plotted in Fig. 4, which with a little difference, are like those in the case study 1. The maximum position(s) for the co-polar and cross-polar component is located at $(x=-0.41a, y=0)$, and $(x=-0.656a, y=\pm 0.708a)$, respectively.

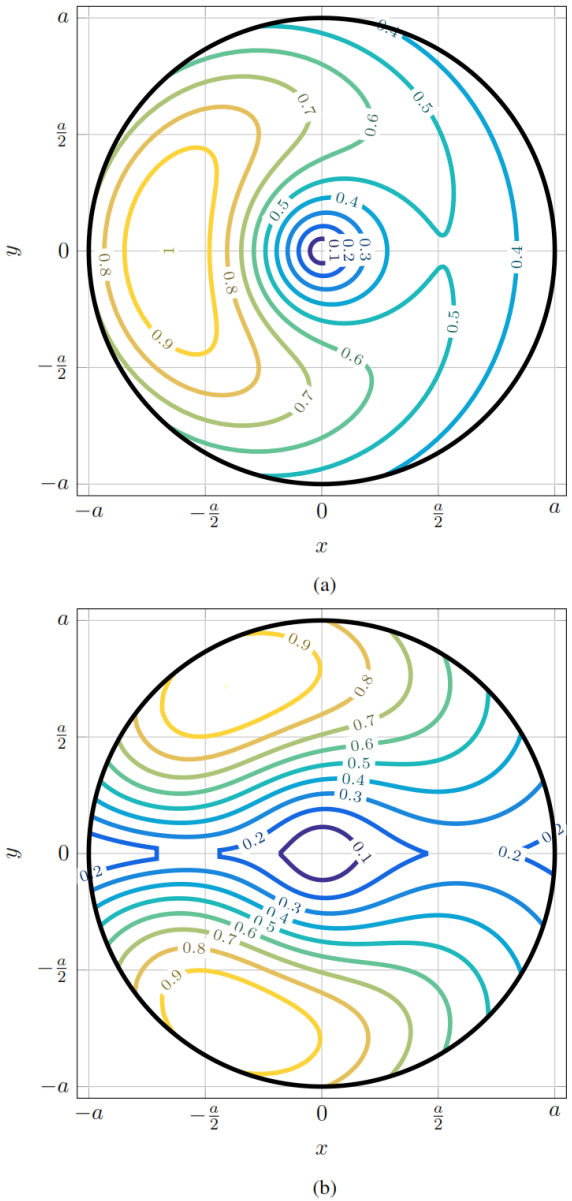

Fig. 3 Normalized variational amplitudes, (a) $\Gamma_{\mathrm{V}}^{2.83^\circ}(t,\psi)$ (b) $\Gamma_{\mathrm{H}}^{2.83^\circ}(t,\psi)$, for case 2.

C. Case study 3

A symmetric center-fed reflector antenna as in [19] is considered for the fourth case study. A left-handed circularly polarized feed antenna with is used to provide the −15dB edge-taper.

The normalized $\Gamma_{\mathrm{R}}^{4.3^\circ}(t,\psi)$ is plotted in Fig. 4. There would be the same contours for left and right-handed polarizations due to the problem symmetry. The contours show that, like two latter cases, the left half of the reflector (lower half in the Fig. 1) has more effect on the radiation in presence of distortions. The maximum position is located at $(x=-0.588a, y=0.094a)$. A little amount of shift is observed in the y-direction which is due to beam squint in the circular polarized offset antennas [20].

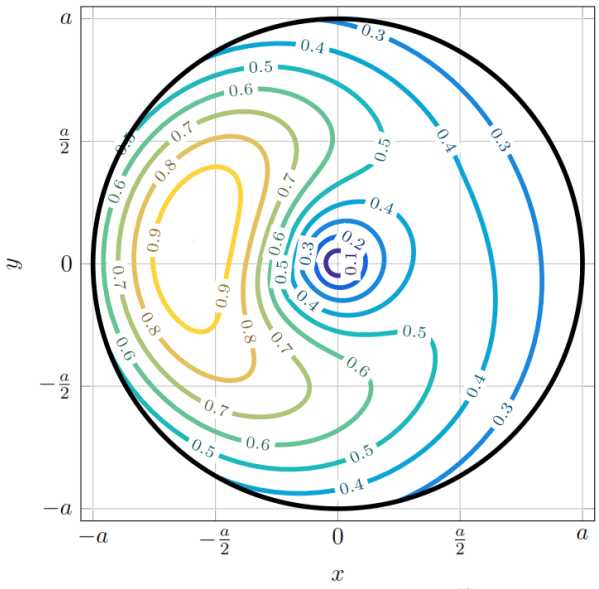

Fig. 4 Normalized variational amplitude, $\Gamma_{\mathrm{R}}^{4.3^\circ}(t,\psi)$ for case 3. Plots for $\Gamma_{\mathrm{L}}^{4.3^\circ}(t,\psi)$ would be the same.

D. Case study 4

An offset reflector antenna is considered as case study 4, which is adapted from [21]. A right-handed circular polarized feed antenna with q=2.8 is used to provide the -20dB edge-taper.

The normalized $\Gamma_{\mathrm{L}}^{6.88^\circ}(t,\psi)$ is plotted in Fig. 5. There are the same contours for left and right-handed polarizations, due to the problem symmetry. Obviously, the contours are symmetric around the center, and the maximum lies on a circle with the radius $0.414a$. Because of the symmetrical feeding system, there are is squint and no shift in the contours.

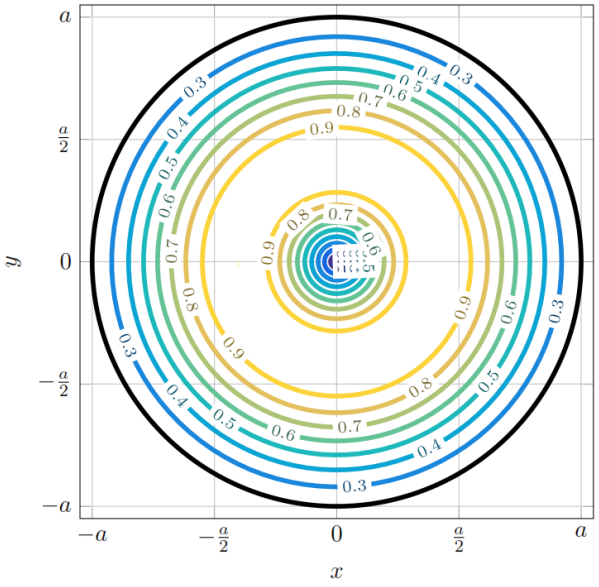

Fig. 5 Normalized variational amplitude, $\Gamma_{\mathrm{L}}^{6.88^\circ}(t,\psi)$ for case 3. Plots for $\Gamma_{\mathrm{R}}^{6.88^\circ}(t,\psi)$ would be the same.

4- Conclusion

In this paper, A new concept of "radiation sensitivity to reflector surface" for reflector antennas was introduced. Different geometries and feeding patterns were studied to extract the sensitivity plots. The plots can be used in practice to control the effects of the surface distortions on the radiation pattern. The functional calculus is used to find the first variational of the radiated field with respect to surface profile function. The variational formula, which is based on PO approximation, can include the normal vector deviations. For a reflector antenna with circular apertures, the variational amplitude plots has been extracted. These plots can be considered as sensitivity contours as they can show the regions with stronger effects on far-field deviations. Different antennas with different geometries and polarizations were dealt with to show the behavior of sensitivity contours. It was noticed that for a single-offset reflector, the surface distortion in the lower half of the surface has more effect on the variations in far-fields. For symmetric reflectors, regions between the center and edges are more important than the center and the edges. Furthermore, in the case of circular polarization, the sensitivity of co- and cross-polarized components of the far-fields have the same behavior.

References

[1] S.K. Sharma, S. Rao, L. Shafai, Handbook of reflector antennas and feed systems volume I: theory and design of reflectors, Artech House, 2013.

[2] G. Cortes-Medellin, P.F. Goldsmith, Analysis of active surface reflector antenna for a large millimeter wave radio telescope, IEEE transactions on antennas and propagation, 42(2) (1994) 176-183.

[3] Y. Rahmat-Samii, Effects of deterministic surface distortions on reflector antenna performance, in: Annales des télécommunications, Springer, 1985, pp. 350-360.

[4] K. Bahadori, Y. Rahmat-Samii, Characterization of effects of periodic and aperiodic surface distortions on membrane reflector antennas, IEEE transactions on antennas and propagation, 53(9) (2005) 2782-2791.

[5] J. Ruze, Antenna tolerance theory—A review, Proceedings of the IEEE, 54(4) (1966) 633-640.

[6] J. Jervase, S. Ghobrial, Axial cross polarization in reflector antennas with surface errors of large correlation diameter, IEEE transactions on antennas and propagation, 31(4) (1983) 662-665.

[7] P. Lian, B. Duan, W. Wang, B. Xiang, N. Hu, Effects of nonuniform surface errors along the radius on reflector's radiation characteristic and its quality evaluation, IEEE Transactions on Antennas and Propagation, 63(5) (2015) 2312-2316.

[8] P. Rocca, N. Anselmi, A. Massa, Interval arithmetic for pattern tolerance analysis of parabolic reflectors, IEEE Transactions on Antennas and Propagation, 62(10) (2014) 4952-4960.

[9] W.T. Smith, R.J. Bastian, An approximation of the radiation integral for distorted reflector antennas using surface-error decomposition, IEEE Transactions on Antennas and Propagation, 45(1) (1997) 5-10.

[10] D.-W. Duan, Y. Rahmat-Samii, A generalized diffraction synthesis technique for high performance reflector antennas, IEEE Transactions on Antennas and Propagation, 43(1) (1995) 27-40.

[11] S. Zhang, B. Duan, H. Bao, P. Lian, Sensitivity analysis of reflector antennas and its application on shaped geo-truss unfurlable antennas, IEEE Transactions on Antennas and propagation, 61(11) (2013) 5402-5407.

[12] J.A. Martinez-Lorenzo, C.M. Rappaport, A.G. Pino, Reflector antenna distortion determination: An iterative-field-matrix solution, Radio Science, 43(4) (2008).

[13] B. Westcott, A. Zaporozhets, Dual-reflector synthesis based on analytical gradient-iteration procedures, IEE Proceedings-Microwaves, Antennas and Propagation, 142(2) (1995) 129-135.

[14] A. Haddadi, A. Ghorbani, Distorted reflector antennas: analysis of radiation pattern and polarization performance, IEEE Transactions on Antennas and Propagation, 64(10) (2016) 4159-4167.

[15] A. Haddadi, P. Taghikhani, A. Ghorbani, A Variational Approach for Modeling Reflector Antenna Surface Distortions Based on Physical Optics Approximation, Antennas and RF Sysems for Space Science, 36th ESA Antenna Workshop on, the Neatherlands, 2015.

[16] P.-S. Kildal, Foundations of antenna engineering: a unified approach for line-of-sight and multipath, Artech House, 2015.

[17] K.W. Cassel, Variational methods with applications in science and engineering, Cambridge University Press, 2013.

Please cite this article using:

A. Haddadi, A. Ghorbani, Distorted Reflector Antennas: Radiation Pattern Sensitivity to the Surface Distortions, *AUT J. Elec. Eng.*, 50(1)(2018) 101-106.

DOI: 10.22060/eej.2017.11922.5016